ORIGINAL RESEARCH
published: 04 May 2021
doi: 10.3389/fmats.2021.670044

MoO_2 Nanospheres Synthesized by Microwave-Assisted Solvothermal Method for the Detection of H_2S in Wide Concentration Range at Low Temperature

Fei An, Shanjun Mu, Shucai Zhang, Wei Xu, Na Li, Haozhi Wang, Shiqiang Wang, Chenyang Zhao, Junjie Feng, Lin Wang and Bing Sun*

State Key Laboratory of Safety and Control for Chemicals, SINOPEC Research Institute of Safety Engineering, Qingdao, China

OPEN ACCESS

Edited by:
Huacheng Zhang,
Xi'an Jiaotong University, China

Reviewed by:
Andrés Juan,
University of Jaume I, Spain
Xinli Xiao,
Harbin Institute of Technology, China

****Correspondence:***
Bing Sun
sunb.qday@sinopec.com

Specialty section:
This article was submitted to Smart Materials, a section of the journal Frontiers in Materials

Received: *20 February 2021*
Accepted: *15 April 2021*
Published: *04 May 2021*

Citation:
An F, Mu S, Zhang S, Xu W, Li N, Wang H, Wang S, Zhao C, Feng J, Wang L and Sun B (2021) MoO_2 Nanospheres Synthesized by Microwave-Assisted Solvothermal Method for the Detection of H_2S in Wide Concentration Range at Low Temperature. Front. Mater. 8:670044. doi: 10.3389/fmats.2021.670044

It is crucial to develop highly energy-efficient and selective sensors for wide concentration range of H_2S, a common toxic gas that widely exists in petrochemical industries. In this work, MoO_2 nanospheres were rapidly synthesized by microwave-assisted solvothermal method, and were subsequently fabricated into H_2S gas sensor. The MoO_2 nanospheres-based sensor exhibited excellent response toward H_2S with good linearity in a wide concentration range (10–240 ppm). Besides, this sensor presented low working temperature, good repeatability, and selectivity against CH_4, H_2, and CO. The outstanding sensing performance results from the reaction between H_2S and abundant chemisorbed oxygen introduced by oxygen vacancies of MoO_2. This result indicates that MoO_2 nanosphere synthesized by microwave-assisted solvothermal method is a promising sensing material for H_2S detection.

Keywords: MoO_2 nanospheres, microwave, solvothermal, H_2S, broad range, gas sensor

INTRODUCTION

H_2S, a common gas in petroleum refining and storage, would cause serious pollution to air and great damage to human body once leaked (Hu et al., 2018). Therefore, the detection and monitoring of H_2S are vital for both environmental conservation and human health. In recent years, different kinds of H_2S sensors have been developed, such as electrochemical sensors, surface acoustic wave sensors and resistive sensors (Mirzaei et al., 2018; Zhao et al., 2018; Khan et al., 2019; Tang et al., 2019). Among them, resistive sensors based on metal oxide nanoparticles have attracted great attention due to the high sensitivity and short recovery time. The metal oxide nanoparticles applied for resistive sensors can be classified into two categories: n-type (ZnO, SnO_2, Fe_2O_3, and MoO_3) and p-type (CuO, Cr_2O_3, and Co_3O_4) semiconductors (Fine et al., 2010; Walker et al., 2019). However, both of them need high operation temperature to achieve good sensing performance, which results in energy consumption issues and gas explosions risks (Gupta Chatterjee et al., 2015). Besides, the detection range of H_2S for current nanoparticle based resistive sensors is mainly around the low end ($<$50 ppm), leading to inaccurate measurement of high concentration H_2S (Guo Y. et al., 2016; Sukunta et al., 2017; Tian et al., 2017).

MoO_2, a n-type semiconductor, has been applied as catalysts, photochromic, and electrochromic materials, due to good electronic conductivity and ion transport property (Ni et al., 2015; Jin et al., 2016; Zhang B. et al., 2017; Xia et al., 2018). However, there have been few reports on H_2S sensors fabricated with MoO_2. The preparation methodology of MoO_2 needs to be improved as well–MoO_2 is usually synthesized by the reduction of MoO_3 with H_2 or CO at ultrahigh temperature, which exhibits enormous risk of explosion (Wang L. et al., 2017; Prabhakar et al., 2018); conventional solvothermal/hydrothermal methods are milder ways to prepare MoO_2, however, the long processing time, additional surfactants and low yield restricts its application (Xiang et al., 2015; Wang et al., 2016; Zhang et al., 2019). Microwave-assisted solvothermal method is a promising alternative method for the preparation of MoO_2. Compared to traditional heat source, microwave irradiation generates a rapid heating to attain the desired temperature, due to the direct heating to polar molecules and conducting ions (Zhu and Chen, 2014). In contrast to the conventional solvothermal/hydrothermal methods, which suffer from large thermal gradients between the inner and outer media, the direct heating provides negligible thermal gradients through the reaction system (Mirzaei and Neri, 2016). The uniform heat distribution is beneficial for preparing regular products. Although MoO_2 nanoparticles prepared with microwave-assisted hydrothermal method has been reported, which still need additional carbon or graphene, the resultant MoO_2 nanoparticles shows irregular morphology (Palanisamy et al., 2015; Fattakhova and Zakharova, 2020). There are few works about MoO_2 nanospheres prepared with microwave-assisted solvothermal method without additional surfactants.

In this report, a new method to synthesize MoO_2 nanospheres without surfactant template by the microwave-assisted solvothermal method was presented. The morphology, crystalline, chemical state and stability of samples were investigated by SEM, XRD, XPS, and TGA. The working temperature, response, repeatability, and selectivity of the gas sensors based on MoO_2 nanospheres were further studied in a gas sensing measurement system. Finally, the gas sensing mechanism of MoO_2 nanospheres was discussed.

EXPERIMENTAL

Materials

$MoCl_5$ was purchased from Sigma-Aldrich (China), absolute ethanol was purchased from Sinopharm (China). All reagents were of analytical grade without further purification, and the deionized water was used in all experiments.

Fabrication of MoO_2 Nanospheres

MoO_2 nanospheres were synthesized by microwave-assisted solvothermal method. In a typical synthesis procedure, 0.57 g of $MoCl_5$ was dissolved in 240 ml absolute ethanol with vigorous stirring for 30 min. The $MoCl_5$ solution was transferred into autoclaves and heated at 200°C for 3 h in a microwave oven (Multiwave PRO, Anton Paar). After cooled to room temperature, the resulting precipitate was collected and washed by centrifuging in deionized water and absolute ethanol, followed by freeze-drying under vacuum for 2 days. The resultant MoO_2 nanospheres were named as MMOs. MMO-180 and MMO-160 were prepared at 180°C and 160°C for 3 h, respectively. For comparison, MoO_2 nanospheres were also synthesized by conventionally solvothermal method, in which the $MoCl_5$ solution was transferred into autoclaves and heated at 200°C for 24 h in an oven. The resultant MoO_2 nanospheres were named as CMOs.

Characterization

A scanning electron microscope (SEM, JEOL JSM-7610F) was used to observe the morphologies of MoO_2. X-ray diffraction (XRD) patterns were obtained on a Bruker D8 Advance Xray diffractometer with a Cu Kα radiation of 0.154 nm at a generator voltage of 40 kV. The chemical compositions of MoO_2 were measured using Thermo Fisher ESCALAB 250 XI X-ray photoelectron spectroscopy (XPS). Thermogravimetric analysis (TGA) was performed in air atmosphere with a heating rate of 10°C/min by using a Shimadzu DTG-60 A thermogravimetric analyzer.

Fabrication and Test of Gas Sensors

The MoO_2 powder was ground and mixed with terpineol at the mass ratio of 1:1 to form a paste. The paste was uniformly coated on the surface of alumina ceramic tube attached with a pair of gold electrodes, which were connected by Pt wires. A Ni-Cr heating wire was inserted into the tube to heat the gas sensor. Before the tests, the sensors were aged at 100°C for 5 days to improve stability. Gas sensing tests were performed on a commercial CGS-8 Gas Sensing Measurement System (Beijing Elite Tech Company Limited) with a test chamber (500 mL in volume). After the sensors' resistance was stabilized at the target temperature, a calculated volume of gas was injected into the chamber. All tests were conducted at a room temperature of 25 ± 5°C and at 40 ± 5% relative humidity.

The gas response is defined as $(R_{air}\text{-}R_{gas})/R_{air}$ (R_{air} and R_{gas} are the sensors' resistance in air and target gas, respectively). The response time and recovery time is defined as the time taken for the response to reach 90% of total change after testing atmosphere changed.

RESULTS AND DISCUSSION

Morphology and Structure

Figure 1 shows the morphology of MoO_2 nanospheres prepared from microwave-assisted and conventional solvothermal method. The diameter of MMOs is in the range of 400–1,000 nm and the average diameter is about 740 nm. In contrast, CMOs own broader distribution of diameter and larger particle size, which affects the homogeneity and sensitivity of gas sensors. Besides, the process of microwave-assisted solvothermal method takes much less time than conventionally solvothermal method, because of the rapid microwave heating (Wang B. et al., 2017). The heating temperature is vital for the regular

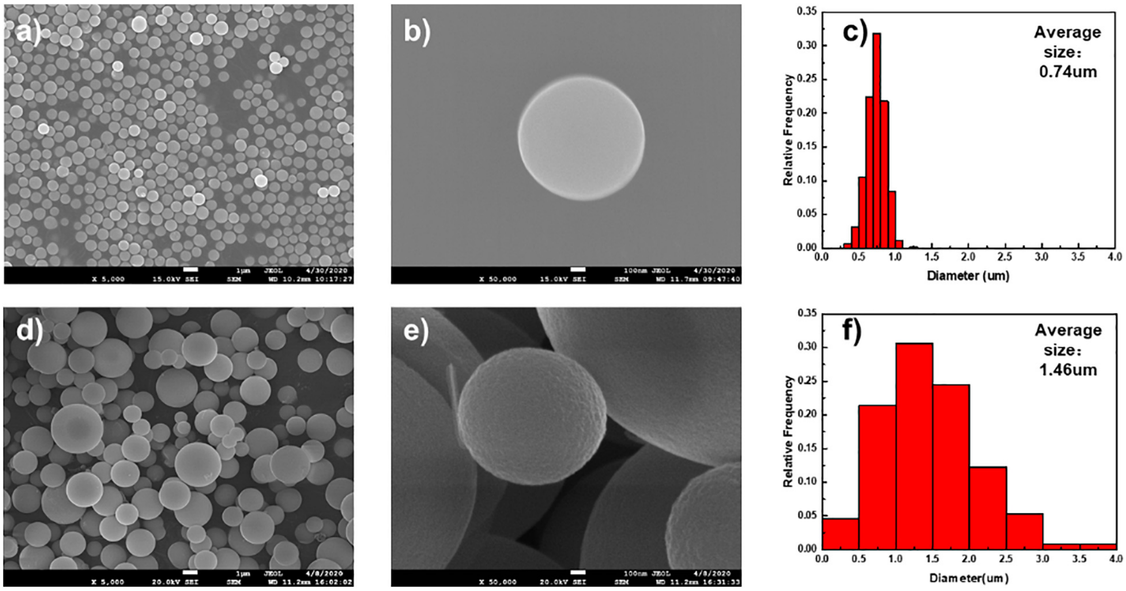

FIGURE 1 | SEM images and diameter statistics of **(a–c)** MMOs and **(d–f)** CMOs.

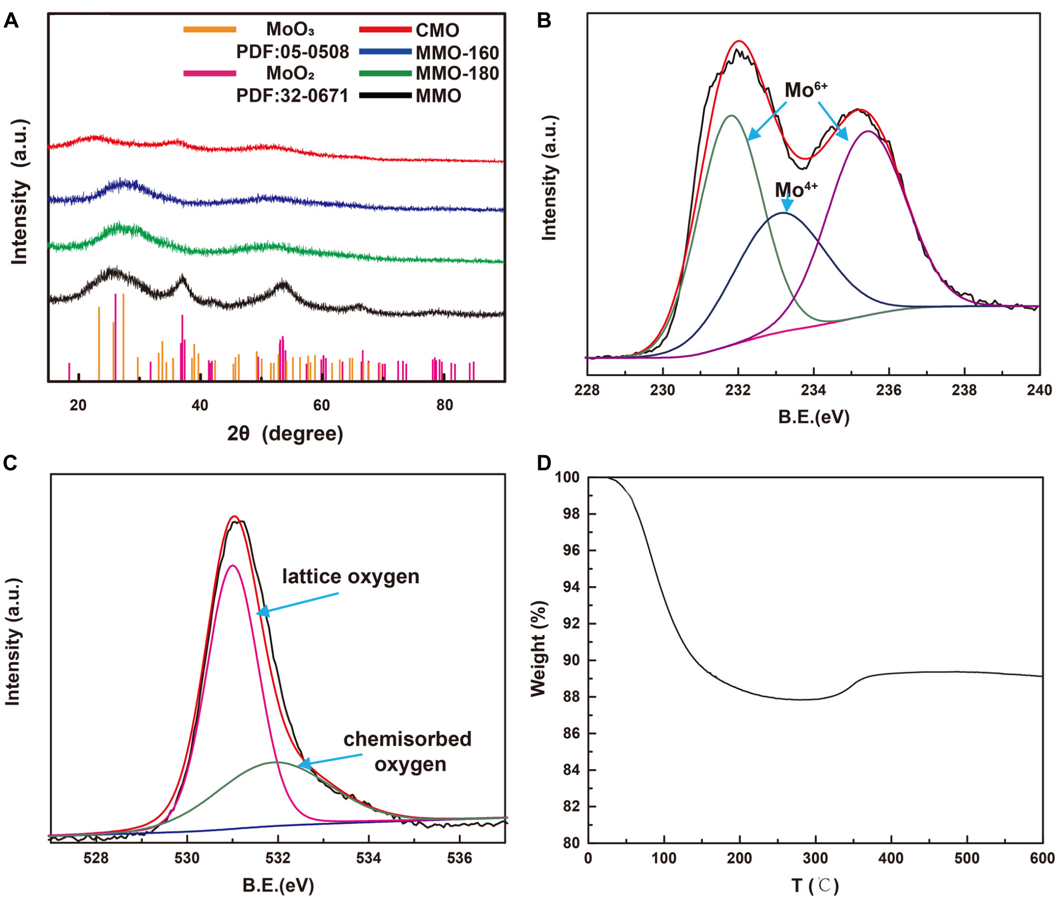

FIGURE 2 | (A) XRD patterns of MMO, MMO-180, MMO-160, and CMO; XPS spectra of **(B)** Mo 3d and **(C)** O1s, and **(D)** TGA curves of MMOs.

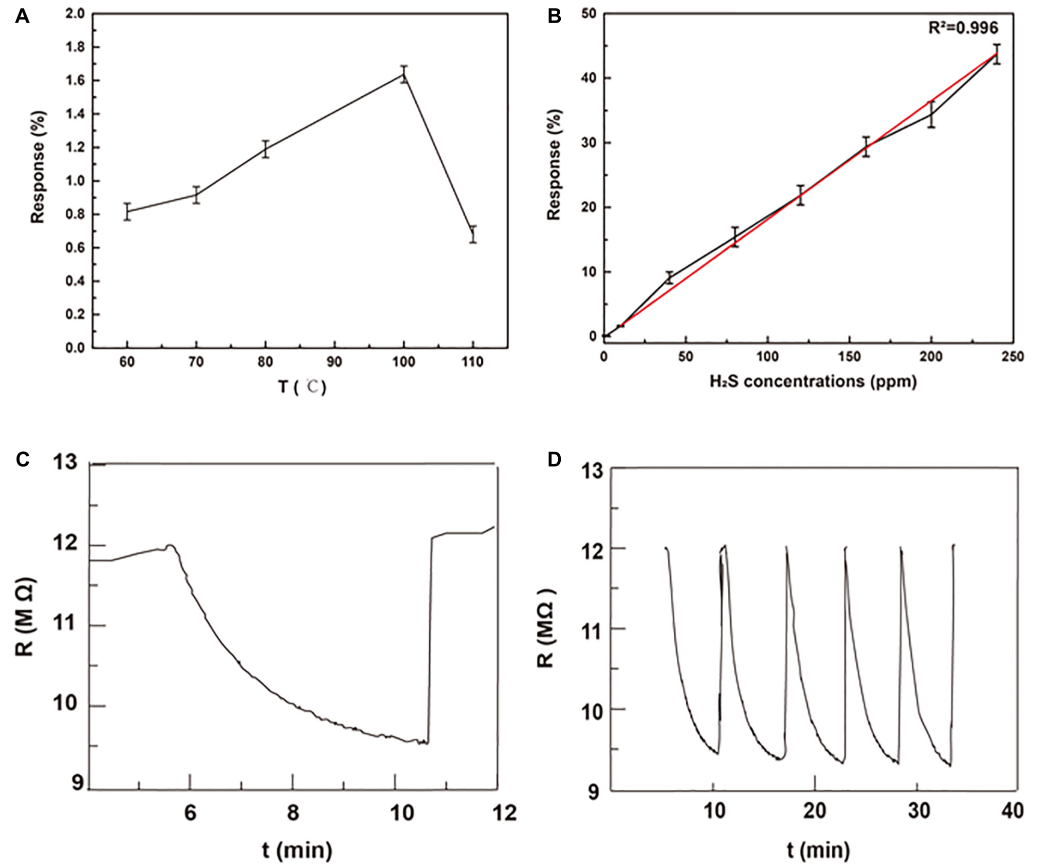

FIGURE 3 | (A) The response of MMOs to 10 ppm H_2S at different working temperature; **(B)** the response of MMOs to different H_2S concentration at 100°C; **(C)** the real-time response of MMOs to 40 ppm H_2S at 100°C; **(D)** five response cycles of MMOs to 40 ppm H_2S at 100°C.

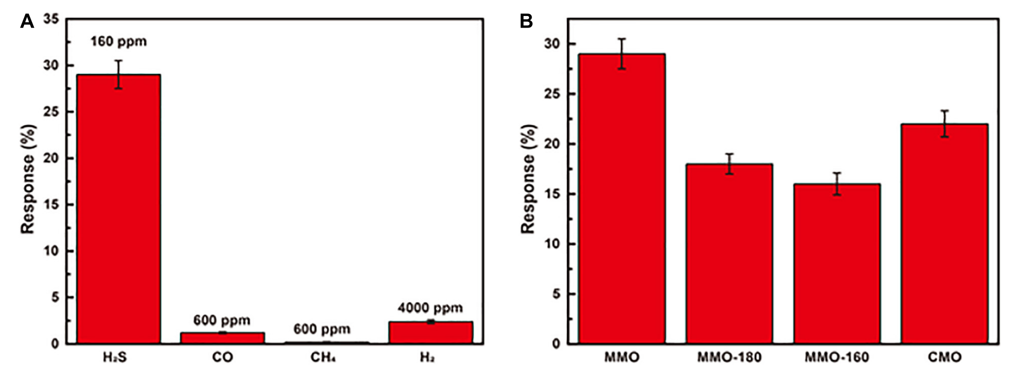

FIGURE 4 | (A) the response of MMOs to various gases; **(B)** the response of MMO, MMO-180, MMO-160, and CMO to 160 ppm H_2S.

morphology of MoO_2 nanospheres during microwave-assisted solvothermal method. As shown in **Supplementary Figure 1**, MMO-180 and MMO-160, prepared at lower temperature, exhibit irregular morphology, which may affect their sensing properties (Cai et al., 2015). Therefore, MMO is chosen to do further characterization and gas tests.

The crystal structure and chemical composition of MMOs were inspected by XRD and XPS. As shown in **Figure 2A**, MMO has distinct diffraction peaks at 2θ = 26.03°, 36.852°, 53.512°, and 66.456°, which could be indexed to (−1 1 1), (1 1 1), (−3 1 2), and (2 0 2) planes of monoclinic MoO_2 phase according to the JCPDS 32-0671 (Kim et al., 2009). This suggests MoO_2 was successfully synthesized by microwave-assisted solvothermal method. On the contrary, MMO-180, MMO-160, and CMO have broader and weaker diffraction peaks, applying to the incomplete crystalline phase, which is consisted with the SEM images. To identify the valence of Mo and the chemisorption of O, we characterized the MMOs by XPS. As shown in **Figure 2B**, XPS spectra of Mo consists of three peaks: two peaks at 231.7 and 235.6 eV present the Mo $3d_{5/2}$ and Mo $3d_{3/2}$ spin-obit components of Mo^{6+}, respectively; the peak at 233.1 eV is assigned to Mo $3d_{5/2}$ of Mo^{4+} (Choi and Thompson, 1996). The appearance of Mo^{6+} indicates the slightly oxidation at the surface of MoO_2 by the exposure to air at room temperature, considering no distinguishing peaks of MoO_3 observed at XRD patterns as shown in **Figure 2A**. **Figure 2C** shows the XPS spectra of O 1 s, consisted of two peaks at 531 and 531.9 eV, corresponding to lattice and chemisorbed oxygen, respectively. The appearance of chemisorbed oxygen results from the coordination unsaturation of Mo, implying the presence of oxygen vacancy (Yang et al., 2015). The abundant chemisorbed oxygen is beneficial for the sensitivity of MoO_2, since the resistance change is mainly occurred by the reaction between chemisorbed oxygen and target gas (Jian et al., 2020). TGA curves of MMO (**Figure 2D**) shows a decrease of mass before 300°C, due to the loss of adsorbed water. During this temperature range, there is no obvious increase of mass, which implies MMOs are relative stable at low temperature. The stability of MMOs at low temperature is crucial for the repeatability of gas sensors. At higher temperature, a slight increase of mass occurred, corresponding to the oxidation of MoO_2.

Gas Sensing Properties

The response to H_2S depends on the physical and chemical absorption of gas, which is strongly affected by the working temperature (Su et al., 2019). Thus, we investigated the optimal working temperature of MMO gas sensor. As shown in **Figure 3A**, the response of MMO gas sensors to 10 ppm H_2S increased first and then decreased as the working temperature rising. The optimal working temperature is 100°C, which is much lower than that of other metal oxide gas sensors and beneficial for energy saving (Guo W. et al., 2016; Wang et al., 2019; Nguyen et al., 2020). The low working temperature may come from the abundant chemisorbed oxygen and oxygen vacancy in MMO (Shen et al., 2019). Therefore, further tests of sensing properties are all completed at 100°C.

TABLE 1 | Comparison of sensing performance between MMO and other metal oxide.

Materials	Optimal working temperature (°C)	Range of H_2S concentration (ppm)	Reference
Pt-WO_3	365	1–5	Kim et al., 2018
Pt-SnO_2	250	1–5	Bulemo et al., 2018
Fe_2O_3/TiO_2	120	1–50	Xu et al., 2019
NiO-SnO_2	200	1–10	Ngoc Hoa et al., 2019
MoO_3	177	1–100	Zhang et al., 2016
SnO_2-CuO	150	1–40	Park et al., 2020
MoO_2	100	1–240	This work

Figure 3B presents the response of MMO to H_2S at different concentrations (1–240 ppm). It can be seen the response increases significantly with increasing concentration of H_2S, and there is good linear relationship (R^2 = 0.996) between response and the concentration of H_2S in the whole range. Unlike other sensors' narrow range of linear relationship, sensors of MMO with good linear relationship in a broad range are suitable for detection of H_2S with large change of concentration (Na et al., 2019; Teng et al., 2020). The response and recovery curve of MMO to 40 ppm H_2S at 100°C is shown in **Figure 3C** with a response time of ∼6 min and recovery time of ∼1 min. The repeatability presented in **Figure 3D** is also important for gas sensors and other devices (Kong et al., 2021a,b). The curves of response

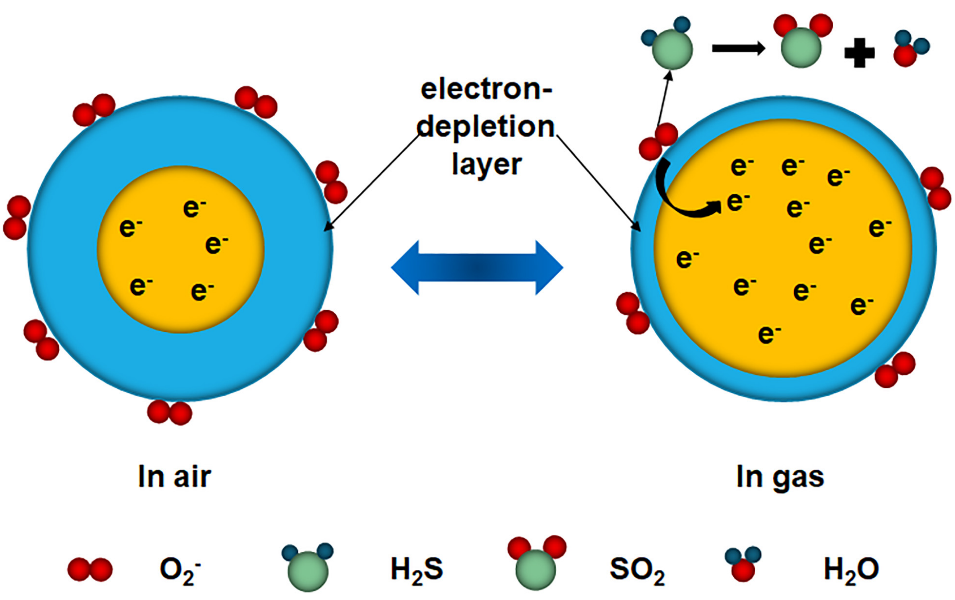

FIGURE 5 | Schematic diagram of H_2S sensing mechanism of MMOs.

show negligible difference after repeating five cycles of tests to 40 ppm H_2S, which implies good repeatability and stability of MMO. To investigate the selectivity of MMO sensor, it was exposed to various gases, including CH_4, H_2, and CO. As shown in **Figure 4A**, the sensor exhibits higher response to H_2S than other gases, which could greatly weaken the interference of non-target gases. The response of MMO, MMO-180, MMO-160, and CMO are shown in **Figure 4B**, in which MMO has the highest response to H_2S.

Table 1 summarizes the sensing performance of different metal oxide to H_2S. Compared to other metal oxide in early work, MMO sensor exhibits lower working temperature and wider concentration range to detect H_2S. Besides, the good repeatability and selectivity makes MMO sensor suitable for detection of H_2S leakage in chemical petrochemical companies.

Gas Sensing Mechanism

As a typical *n*-type semiconductor, the sensing performance of MMO strongly depends on the free electron density (**Figure 5**). According to the density functional theory (DFT), the adsorption and dissociation of O_2 on MoO_2 surface could occur rapidly at room temperature, due to the high adsorption energy and low dissociation barrier (Zhang Q. et al., 2017). Therefore, when MMO exposed to air, oxygen molecules adsorb onto the surface of MMO and take free electrons from MMO, forming chemisorbed oxygen ($O_2{}^-$) and resistant electron-depletion layer (EDL) as the working temperature below 150°C (Franke et al., 2006). This leads to decreased free electron density and increased resistance (Mirzaei et al., 2018). After H_2S was injected into the chamber, H_2S molecules react with $O_2{}^-$ to form SO_2 and water vapor. In this process, free electrons trapped by $O_2{}^-$ come back to the MMO, causing the increased free electron density and decreased resistance (Katoch et al., 2015). After exposed to air again, the oxygen molecules will be re-adsorbed and reconstruct the EDL. During the tests, H_2O also participated in the reaction *via* reacting with hole (h^+) to render the radical hydroxyl(•OH), which justifies the optimal working temperature is 100°C.

The whole reaction is described below:

$$O_2(g) \leftrightarrow O_2(ad)$$

$$O_2(ad) + e^- \rightarrow O_2{}^-(ad)$$

$$2H_2S + 3O_2{}^-(ad) \rightarrow 2SO_2 + 2H_2O + 3e^-$$

$$H_2O(ad) + h^+ \rightarrow \bullet OH + H^+$$

As discussed in XPS characterization before, there is abundant chemisorbed oxygen on the surface of MMO, which could react with a large of H_2S molecules without saturation. This causes the good linear relationship in a broad range of MMO sensors to H_2S.

CONCLUSION

MoO_2 nanospheres was rapidly synthesized by microwave-assisted solvothermal method at 200°C for 3 h. The resultant MMO exhibit more regular dimension than CMON prepared by conventionally solvothermal method. At an optical working temperature of 100°C, the MMO-based sensors exhibit excellent response, linear relationship, repeatability and selectivity toward a broad concentration range of H_2S (10–240 ppm). The oxygen vacancies on the surface of MMO results in abundant chemisorbed oxygen which could react with H_2S, causing outstanding sensing performance of MMO sensors. In a word, MoO_2 nanosphere with abundant chemisorbed oxygen is a promising sensing material for detection of H_2S leakage in chemical companies.

DATA AVAILABILITY STATEMENT

The original contributions presented in the study are included in the article/**Supplementary Material**, further inquiries can be directed to the corresponding author/s.

AUTHOR CONTRIBUTIONS

FA, SM, BS, and SZ contributed to conception and design of the study. WX organized the database. NL performed the statistical analysis. HW wrote the first draft of the manuscript. SW, CZ, JF, and LW wrote sections of the manuscript. All authors contributed to manuscript revision, read, and approved the submitted version.

FUNDING

Financial support from the National Natural Science Foundation of China (52003297) is gratefully acknowledged.

SUPPLEMENTARY MATERIAL

The Supplementary Material for this article can be found online at: https://www.frontiersin.org/articles/10.3389/fmats.2021.670044/full#supplementary-material

Supplementary Figure 1 | SEM images of **(A,B)** MMO-180 and **(C,D)** MMO-160.

REFERENCES

Bulemo, P. M., Cho, H. J., Kim, D. H., and Kim, I. D. (2018). Facile synthesis of Pt-functionalized meso/macroporous SnO_2 hollow spheres through in situ templating with SiO_2 for H_2S sensors. *ACS Appl. Mater. Interfaces* 10, 18183–18191. doi: 10.1021/acsami.8b00901

Cai, Z.-X., Yang, X.-N., Li, H.-Y., and Guo, X. (2015). NO sensing by single crystalline WO_3 nanowires. *Sens. Actuators B* 219, 346–353. doi: 10.1016/j.snb.2015.05.036

Choi, J. G., and Thompson, L. T. (1996). XPS study of as-prepared and reduced molybdenum oxides. *Appl. Surf. Sci.* 93, 143–149. doi: 10.1016/0169-4332(95)00317-7

Fattakhova, Z. A., and Zakharova, G. Z. (2020). MoO_2/C composites: synthesis, properties, and formation mechanism. *Russ. J. Inorg. Chem.* 65, 480–487. doi: 10.1134/S0036023620040051

Fine, G. F., Cavanagh, L. M., Afonja, A., and Binions, R. (2010). Metal oxide semiconductor gas sensors in environmental monitoring. *Sensors* 10, 5469–5502. doi: 10.3390/s100605469

Franke, M., Koplin, T., and Simon, U. (2006). Metal and metal oxide nanoparticles in chemiresistors: does the nanoscale matter? *Small* 2, 36–50. doi: 10.1002/smll.200500261

Guo, W., Mei, L., Wen, J., and Ma, J. (2016). High-response H_2S sensor based on ZnO/SnO_2 heterogeneous nanospheres. *RSC Adv.* 6, 15048–15053. doi: 10.1039/C5RA22187K

Guo, Y., Gong, M., Li, Y., Liu, Y., and Dou, X. (2016). Sensitive, selective, and fast detection of ppb-level H_2S gas boosted by ZnO-CuO mesocrystal. *Nanoscale Res. Lett.* 11:475. doi: 10.1186/s11671-016-1688-y

Gupta Chatterjee, S., Chatterjee, S., Ray, A. K., and Chakraborty, A. K. (2015). Graphene–metal oxide nanohybrids for toxic gas sensor: a review. *Sens. Actuators B* 221, 1170–1181. doi: 10.1016/j.snb.2015.07.070

Hu, X., Zhu, Z., Li, Z., Xie, L., Wu, Y., and Zheng, L. (2018). Zheng, heterostructure of CuO microspheres modified with $CuFe_2O_4$ nanoparticles for highly sensitive H_2S gas sensor. *Sens. Actuators B* 264, 139–149. doi: 10.1016/j.snb.2018.02.110

Jian, Y., Hu, W., Zhao, Z., Cheng, P., Haick, H., Yao, M., et al. (2020). Gas sensors based on chemi-resistive hybrid functional nanomaterials. *Nano Micro Lett.* 12:71. doi: 10.1007/s40820-020-0407-5

Jin, Y., Wang, H., Li, J., Yue, X., Han, Y., Shen, P. K., et al. (2016). Porous MoO_2 nanosheets as non-noble bifunctional electrocatalysts for overall water splitting. *Adv. Mater.* 28, 3785–3790. doi: 10.1002/adma.201506314

Katoch, A., Choi, S. W., Kim, J. H., Lee, J. H., Lee, J. S., and Sang, S. K. (2015). Importance of the nanograin size on the H_2S-sensing properties of ZnO–CuO composite nanofibers. *Sens. Actuators B* 214, 111–116. doi: 10.1016/j.snb.2015.03.012

Khan, M., Rao, M., and Li, Q. (2019). Recent advances in electrochemical sensors for detecting toxic gases: NO_2, SO_2 and H_2S. *Sensors* 19:905. doi: 10.3390/s19040905

Kim, M. H., Jang, J. S., Koo, W. T., Choi, S. J., Kim, S. J., Kim, D. H., et al. (2018). Bimodally porous WO_3 microbelts functionalized with Pt catalysts for selective H_2S sensors. *ACS Appl. Mater. Interfaces* 10, 20643–20651. doi: 10.1021/acsami.8b00588

Kim, W.-S., Kim, H.-C., and Hong, S.-H. (2009). Gas sensing properties of MoO_3 nanoparticles synthesized by solvothermal method. *J. Nanopar. Res.* 12, 1889–1896. doi: 10.1007/s11051-009-9751-6

Kong, D., Li, J., Guo, A., and Xiao, X. (2021a). High temperature electromagnetic shielding shape memory polymer composite. *Chem. Eng. J.* 408:127365. doi: 10.1016/j.cej.2020.127365

Kong, D., Li, J., Guo, A., Yu, J., and Xiao, X. (2021b). Smart polyimide with recovery stress at the level of high temperature shape memory alloys. *Smart Mater. Strut.* 30:035027. doi: 10.1088/1361-665X/abe182

Mirzaei, A., Kim, S. S., and Kim, H. W. (2018). Resistance-based H_2S gas sensors using metal oxide nanostructures: a review of recent advances. *J. Hazard. Mater.* 357, 314–331. doi: 10.1016/j.jhazmat.2018.06.015

Mirzaei, A., and Neri, G. (2016). Microwave-assisted synthesis of metal oxide nanostructures for gas sensing application: a review. *Sens. Actuators B* 237, 749–775. doi: 10.1016/j.snb.2016.06.114

Na, H.-B., Zhang, X.-F., Zhang, M., Deng, Z.-P., Cheng, X.-L., Huo, L.-H., et al. (2019). A fast response/recovery ppb-level H_2S gas sensor based on porous CuO/ZnO heterostructural tubule via confined effect of absorbent cotton. *Sens. Actuators B* 297, 126816–126826. doi: 10.1016/j.snb.2019.126816

Ngoc Hoa, T. T., Hoa, N. D., Van Duy, N., Hung, C. M., Thanh Le, D. T., Van Toan, N., et al. (2019). An effective H_2S sensor based on SnO_2 nanowires decorated with NiO nanoparticles by electron beam evaporation. *RSC Adv.* 9, 13887–13895. doi: 10.1039/C9RA01105F

Nguyen, H. T. T., Truong, T. H., Nguyen, T. D., Dang, V. T., Vu, T. V., Nguyen, S. T., et al. (2020). Ni-doped WO_3 flakes-based sensor for fast and selective detection of H_2S. *J. Mater. Sci. Mater. Electron.* 31, 12783–12795. doi: 10.1007/s10854-020-03830-9

Ni, J., Zhao, Y., Li, L., and Mai, L. (2015). Ultrathin MoO_2 nanosheets for superior lithium storage. *Nano Energy* 11, 129–135. doi: 10.1016/j.nanoen.2014.10.027

Palanisamy, K., Kim, Y., Kim, H., Kim, J. M., and Yoon, W. S. (2015). Self-assembled porous MoO_2/graphene microspheres towards high performance anodes for lithium ion batteries. *J. Power Sour.* 275, 351–361. doi: 10.1016/j.jpowsour.2014.11.001

Park, K.-R., Cho, H.-B., Lee, J., Song, Y., Kim, W.-B., and Choa, Y.-H. (2020). Design of highly porous SnO_2-CuO nanotubes for enhancing H_2S gas sensor performance. *Sens. Actuators B* 302, 127179–127185. doi: 10.1016/j.snb.2019.127179

Prabhakar, R. K., Mhamane, N. B., Kumar, G. M., and Gopinath, C. S. (2018). Mapping valence band and interface electronic structure changes during oxidation of Mo to MoO_3 via MoO_2 and MoO_3 reduction to MoO_2: a nappes study. *J. Phys. Chem. C* 122, 23034–23044. doi: 10.1021/acs.jpcc.8b07024

Shen, S., Zhang, X., Cheng, X., Xu, Y., Gao, S., Zhao, H., et al. (2019). Oxygen-vacancy-enriched porous α-MoO_3 nanosheets for trimethylamine sensing. *ACS Appl. Nano Mater.* 2, 8016–8026. doi: 10.1021/acsanm.9b02072

Su, Y., Chen, P., Wang, P., Ge, J., Hu, S., Zhao, Y., et al. (2019). Pd-loaded SnO_2 hierarchical nanospheres for a high dynamic range H_2S micro sensor. *RSC Adv.* 9, 5987–5994. doi: 10.1039/C8RA09156K

Sukunta, J., Wisitsoraat, A., Tuantranont, A., Phanichphant, S., and Liewhiran, C. (2017). Highly-sensitive H_2S sensors based on flame-made V-substituted SnO_2 sensing films. *Sens. Actuators B* 242, 1095–1107. doi: 10.1016/j.snb.2016.09.140

Tang, Q. B., Guo, Y. J., Tang, Y. L., Long, G. D., Wang, J. L., Li, D. J., et al. (2019). Highly sensitive and selective love mode surface acoustic wave ammonia sensor based on graphene oxides operated at room temperature. *J. Mater. Sci.* 54, 11925–11935. doi: 10.1007/s10853-019-03764-6

Teng, Y., Zhang, X.-F., Xu, T.-T., Deng, Z.-P., Xu, Y.-M., Huo, L.-H., et al. (2020). A spendable gas sensor with higher sensitivity and lowest detection limit towards H_2S: porous α-Fe_2O_3 hierarchical tubule derived from poplar branch. *Chem. Eng. J.* 392, 123679–123688. doi: 10.1016/j.cej.2019.123679

Tian, K., Wang, X. X., Yu, Z. Y., Li, H. Y., and Guo, X. (2017). Hierarchical and hollow Fe_2O_3 nanoboxes derived from metal-organic frameworks with excellent sensitivity to H_2S. *ACS Appl. Mater. Interfaces* 9, 29669–29676. doi: 10.1021/acsami.7b07069

Walker, J. M., Akbar, S. A., and Morris, P. A. (2019). Synergistic effects in gas sensing semiconducting oxide nano-heterostructures: a review. *Sens. Actuators B* 286, 624–640. doi: 10.1016/j.snb.2019.01.049

Wang, B., He, J., Liu, F., and Ding, L. (2017). Rapid synthesis of Cu_2O/CuO/rGO with enhanced sensitivity for ascorbic acid biosensing. *J. Alloys Compd.* 693, 902–908. doi: 10.1016/j.jallcom.2016.09.291

Wang, L., Bu, C.-Y., Zhang, G.-H., Wang, J.-S., and Chou, K.-C. (2017). Study of the reduction of industrial grade MoO_3 powders with CO or CO-CO_2 gases to prepare MoO_2. *Metall. Mater. Trans. B* 48, 2047–2056. doi: 10.1007/s11663-017-0979-8

Wang, P., Hui, J., Yuan, T., Chen, P., Su, Y., Liang, W., et al. (2019). Ultrafine nanoparticles of W-doped SnO_2 for durable H_2S sensors with fast response and recovery. *RSC Adv.* 9, 11046–11053. doi: 10.1039/C9RA00944B

Wang, Y., Yu, L., and Lou, X. W. (2016). Formation of triple-shelled molybdenum-polydopamine hollow spheres and their conversion into MoO_2/carbon composite hollow spheres for lithium-ion batteries. *Angew. Chem.* 55, 14668–14672. doi: 10.1002/anie.201608410

Xia, C., Zhou, Y., Velusamy, D. B., Farah, A. A., Li, P., Jiang, Q., et al. (2018). Anomalous Li storage capability in atomically thin two-dimensional sheets of nonlayered MoO_2. *Nano Lett.* 18, 1506–1515. doi: 10.1021/acs.nanolett.7b05298

Xiang, Z., Zhang, Q., Zhang, Z., Xu, X., and Wang, Q. (2015). Preparation and photoelectric properties of semiconductor MoO_2 micro/nanospheres with wide bandgap. *Ceram. Int.* 41, 977–981. doi: 10.1016/j.ceramint.2014.09.017

Xu, Z., Liu, H., Tong, X., Shen, W., Chen, X., and Bloch, J.-F. (2019). A low operating temperature and high performance sensor for H_2S detection based on α-Fe_2O_3/TiO_2 heterojunction nanoparticles composite. *J. Mater. Sci. Mater. Electron.* 30, 12695–12709. doi: 10.1007/s10854-019-01634-0

Yang, S., Wang, Z., Hu, Y., Luo, X., Lei, J., Zhou, D., et al. (2015). Highly responsive room-temperature hydrogen sensing of alpha-MoO_3 nanoribbon membranes. *ACS Appl. Mater. Interfaces* 7, 9247–9253. doi: 10.1021/acsami.5b01858

Zhang, B., Xue, Y., Jiang, A., Xue, Z., Li, Z., and Hao, J. (2017). Ionic liquid as reaction medium for synthesis of hierarchically structured one-dimensional

MoO_2 for efficient hydrogen evolution. *ACS Appl. Mater. Interfaces* 9, 7217–7223. doi: 10.1021/acsami.7b00722

Zhang, L., Liu, Z., Jin, L., Zhang, B., Zhang, H., Zhu, M., et al. (2016). Self-assembly gridding α-MoO_3 nanobelts for highly toxic H_2S gas sensors. *Sens. Actuators B* 237, 350–357. doi: 10.1016/j.snb.2016.06.104

Zhang, Q., Zhang, M., and Wiltowski, T. (2017). Adsorption and dissociation of O_2 on MoO_2(111) surfaces: a DFT study. *Phys. Chem. Chem. Phys.* 43, 29244–29254. doi: 10.1039/C7CP06456J

Zhang, W., Wang, B., Luo, H., Jin, F., Ruan, T., and Wang, D. (2019). MoO_2 nanobelts modified with an MOF-derived carbon layer for high performance lithium-ion battery anodes. *J. Alloys Compd.* 803, 664–670. doi: 10.1016/j.jallcom.2019.06.337

Zhao, Y., Yang, Y., Cui, L., Zheng, F., and Song, Q. (2018). Electroactive Au@Ag nanoparticles driven electrochemical sensor for endogenous H_2S detection. *Biosens. Bioelectron.* 117, 53–59. doi: 10.1016/j.bios.2018.05.047

Zhu, Y. J., and Chen, F. (2014). Microwave-assisted preparation of inorganic nanostructures in liquid phase. *Chem. Rev.* 114, 6462–6555. doi: 10.1021/cr400366s

Conflict of Interest: The authors declare that the research was conducted in the absence of any commercial or financial relationships that could be construed as a potential conflict of interest.